ESC European Society of Cardiology

Cardiovascular Research (2021) **117**, 792–804
doi:10.1093/cvr/cvaa089

Ryanodine receptor subtypes regulate Ca^{2+} sparks/spontaneous transient outward currents and myogenic tone of uterine arteries in pregnancy

Rui Song, Xiang-Qun Hu , Monica Romero, Mark A. Holguin, Whitney Kagabo , Daliao Xiao , Sean M. Wilson, and Lubo Zhang*

Lawrence D. Longo, MD Center for Perinatal Biology, Department of Basic Sciences, Loma Linda University School of Medicine, Loma Linda, CA 92350, USA

Received 21 August 2019; revised 18 February 2020; editorial decision 31 March 2020; accepted 31 March 2020; online publish-ahead-of-print 6 April 2020

Time for primary review: 32 days

Aims Our recent study demonstrated that increased Ca^{2+} sparks and spontaneous transient outward currents (STOCs) played an important role in uterine vascular tone and haemodynamic adaptation to pregnancy. The present study examined the role of ryanodine receptor (RyR) subtypes in regulating Ca^{2+} sparks/STOCs and myogenic tone in uterine arterial adaptation to pregnancy.

Methods and results Uterine arteries isolated from non-pregnant and near-term pregnant sheep were used in the present study. Pregnancy increased the association of α and β1 subunits of large-conductance Ca^{2+}-activated K^+ (BK_{Ca}) channels and enhanced the co-localization of RyR1 and RyR2 with the β1 subunit in the uterine artery. In contrast, RyR3 was not co-localized with BK_{Ca} β1 subunit. Knockdown of RyR1 or RyR2 in uterine arteries of pregnant sheep downregulated the β1 but not α subunit of the BK_{Ca} channel and decreased the association of α and β1 subunits. Unlike RyR1 and RyR2, knockdown of RyR3 had no significant effect on either expression or association of BK_{Ca} subunits. In addition, knockdown of RyR1 or RyR2 significantly decreased Ca^{2+} spark frequency, suppressed STOCs frequency and amplitude, and increased pressure-dependent myogenic tone in uterine arteries of pregnant animals. RyR3 knockdown did not affect Ca^{2+} sparks/STOCs and myogenic tone in the uterine artery.

Conclusion Together, the present study demonstrates a novel mechanistic paradigm of RyR subtypes in the regulation of Ca^{2+} sparks/STOCs and uterine vascular tone, providing new insights into the mechanisms underlying uterine vascular adaptation to pregnancy.

* Corresponding author. Tel: 909 558 4325; fax: 909 558 4029, E-mail: lzhang@llu.edu

Graphical Abstract

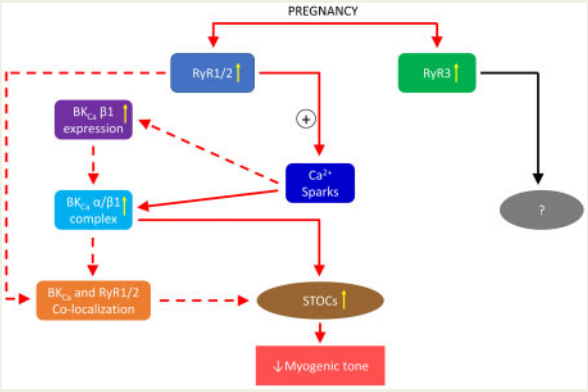

Keywords Pregnancy • Uterine arteries • Ryanodine receptor • Large-conductance Ca^{2+}-activated K+ • channel • Ca^{2+} sparks • Spontaneous transient outward currents • Myogenic tone

1. Introduction

To accommodate the demand of foetal growth during pregnancy, uterine vascular tone reduces substantially and uterine blood flow increases dramatically.[1] Uterine vascular adaptation has been extensively studied, and yet the mechanisms underlying this phenomenon remain not fully understood. Previous studies have demonstrated that upregulation of the β1 subunit (BK_{Ca} β1) of the large-conductance Ca^{2+}-activated K^+ channel and enhanced channel function in uterine arteries are essential for reduced uterine vascular tone and increased uterine blood flow.[2–7] Under physiological conditions, the activity of BK_{Ca} channels in vascular smooth muscle cells is stimulated by ryanodine receptor (RyR)-mediated Ca^{2+} sparks and exists in the form of spontaneous transient outward currents (STOCs). The K^+ efflux carried by STOCs promotes vascular smooth muscle cell membrane hyperpolarization and subsequent closure of L-type voltage-gated Ca^{2+} ($Ca_V1.2$) channels, leading to vasorelaxation.[8] The functional coupling between RyRs and BK_{Ca} channels is highly efficient that virtually a one-to-one relationship exists between Ca^{2+} sparks and STOCs.[9] The regulation of vascular tone by the Ca^{2+} spark-STOC coupling has been frequently observed in vascular beds of cerebral and mesenteric circulations.[10–14] We have recently revealed that pregnancy attenuates myogenic tone in uterine arteries by promoting Ca^{2+} spark-STOC coupling in uterine arteries, providing a novel mechanism underlying the uterine vascular adaptation.[15]RyRs consist of three subtypes: RyR1, RyR2, and RyR3. All of them are expressed in smooth muscle cells.[16] Consistently, uterine arteries also express all RyR subtypes.[15] Both RyR1 and RyR2 have been shown to contribute to the generation of Ca^{2+} sparks.[17–19] However, RyR3 was found either not to initiate Ca^{2+} sparks or to negatively regulate Ca^{2+} spark generation.[17,20] The sarcoplasmic reticulum runs parallel with the plasma membrane and they stay close to each other. This structural arrangement permits a close interaction between RyRs in the sarcoplasmic reticulum membrane and BK_{Ca} channels in the plasma membrane. It is estimated that activation of the BK_{Ca} channel by Ca^{2+} requires the channel being located within 10–30 nm of RyRs.[21] Interestingly, a Ca^{2+} microdomain created by Ca^{2+} sparks may cover a radius of ~200 nm.[22] BK_{Ca} β1 residing within the spatial boundaries of the Ca^{2+} microdomain could then function as a Ca^{2+} sensor and transmit the Ca^{2+} signal to the BK_{Ca} channel, leading to increased BK_{Ca} channel activity.[23,24] Importantly, the spatial organization of RyRs and BK_{Ca} channels is critical for the Ca^{2+} spark-STOC coupling.[25,26]

Our recent study revealed that all three subtypes of RyRs were upregulated in uterine arteries during pregnancy, and the upregulation of RyRs conferred pregnancy-induced increases in Ca^{2+} spark activity and STOCs and reduction in uterine arterial myogenic tone.[15] A question of great importance that needs to be addressed is which subtype(s) of RyRs and its spatial organization with the BK_{Ca} channel contribute to the enhanced Ca^{2+} spark-STOC coupling in uterine arteries in pregnancy. Herein, we present evidence that pregnancy promotes co-localization of RyR1 and RyR2 with BK_{Ca} β1, leading to the upregulation of Ca^{2+} spark activity and STOCs and attenuation of myogenic tone in uterine arteries. Moreover, RyR1 and RyR2 also play a role in regulating the expression of BK_{Ca} β1and its association with the BK_{Ca} channel α subunit (BK_{Ca} α) in uterine arteries. These findings provide novel insights into the mechanisms underlying the physiological adaptation of uterine vasculature during pregnancy.

2. Methods

2.1 Tissue preparation and treatment

All procedures and protocols were approved by the Institutional Animal Care and Use Committee of Loma Linda University and followed the guidelines by the National Institutes of Health Guide for the Care and Use of Laboratory Animals. Tissue collection was carried out under anaesthesia. After tissue collection, animals were killed via intravenous injection of 15 mL T-61 solution (Hoechst-Rousel, Somerville, NJ, USA), according to American Veterinary Medical Association guidelines.

Uterine arteries were harvested from non-pregnant or near-term (~142–145 days of gestation) pregnant sheep.[27] Animals were anaesthetized with intravenous injection of propofol (2 mg/kg) followed by intubation, and anaesthesia was maintained on 1.5–3.0% isoflurane balanced

in O_2 throughout the surgery. An incision was made in the abdomen, and the uterus was exposed. Resistance-sized uterine arteries (~150–200 μm in diameter) were used in all experiments. Arteries were isolated and removed without stretching and placed into a physiological salt solution (PSS) containing (in mmol/L) 130.0 NaCl, 10.0 HEPES, 6.0 glucose, 4.0 KCl, 4.0 $NaHCO_3$, 1.8 $CaCl_2$, 1.2 $MgSO_4$, 1.18 KH_2PO_4, and 0.025 EDTA (pH 7.4). To knockdown RyRs, resistance-sized uterine arteries of pregnant sheep were transfected with RyR siRNAs (Dharmacon Inc., Lafayette, CO, USA) as described previously.[6] Target or scrambled siRNAs were mixed with HiPerfect Transfection Reagent (Qiagen) and Opti-MEM I (ThermoFisher) for 30–45 min at room temperature and subsequently added into DMEM/F12 supplemented with 1% charcoal-stripped foetal bovine serum. Tissues were incubated with the medium containing target or scrambled siRNAs (control siRNA, the final concentration of 200 nmol/L) in an incubator at 37°C for 48 h.

2.2 Real-time RT-PCR

Total RNA was isolated using TRIzol reagent (Thermo Fisher) and subjected to reverse transcription with iScript cDNA Synthesis system (Bio-Rad, Hercules, CA, USA). The mRNA abundance of RyRs was measured with real-time polymerase chain reaction (PCR) using iQ SYBR Green Supermix (Bio-Rad), as described previously.[28] Primers used were 5′-CAGAGGGGGAAAAAGAGGAC-3′ (forward) and 5′-ACGGTGCTGTAGCTCTTGGT-3′ (reverse) for RyR1, 5′-TGAGG CTCACAGGCTTTTCT-3′ (forward) and 5′-ATGCAGGGGATAC AGGTTTG-3′ (reverse) for RyR2, and 5′-TAAAGTATGGGCCCG AAGTG-3′ (forward) and 5′-TTTCATTTCTGCTGCCTGTG-3′ (reverse) for RyR3. Ribosomal protein L4 (RPL4) content in uterine arteries was not altered by pregnancy[15] and was used for normalization of the abundance of mRNAs. PCR was performed in triplicate, and threshold cycle numbers (C_T), generated by CFX connect Real-time System (Bio-Rad), were averaged for each sample. The RNA quality was assessed by a Nanodrop Spectrophotometer (ThermoFisher) by determining A260/A280, A260/A230 values. The relative gene expression of the gene of interest (GOI) was calculated by the modified $2_T^{-\Delta\Delta C}$ method.[29]

2.3 Immunoblotting

Protein abundance of RyR1, RyR2, and RyR3 in uterine arteries was measured as described previously.[5] Briefly, tissues were homogenized in a lysis buffer followed by centrifugation at 4°C for 10 min at 10 000 *g*, and the supernatants were collected. Samples with equal proteins were loaded onto NuPAGE 3–8% Tris-Acetate Protein Gels (Thermo Fisher Scientific, Waltham, MA, USA) and were separated by electrophoresis at 150 V for 1 H. Proteins were then transferred onto nitrocellulose membranes. After blocking non-specific binding sites by dry milk, membranes were incubated with primary antibodies (1:1000 dilution) against rabbit polyclonal RyR1 (8153, Cell Signaling, Danvers, MA, USA), rabbit polyclonal RyR2 (ARR-002, Alomone Labs, Israel), rabbit polyclonal RyR3 (AB9082, EMD Millipore), mouse monoclonal BK_{Ca} channel α, or mouse monoclonal BK_{Ca} channel β1 (Santa Cruz Biotechnology, Dallas, TX, USA). After washing, membranes were incubated with secondary horseradish peroxidase-conjugated antibodies. Proteins were visualized with enhanced chemiluminescence reagents, and blots were exposed to Hyperfilm. Results were quantified with the Kodak electrophoresis documentation and analysis system and Kodak ID image analysis software (Kodak, Rochester, NY, USA). The target protein abundance was normalized to the abundance of β-actin as a protein loading control, whose abundance in uterine arteries was not altered by pregnancy.[15]

2.4 Ca^{2+} spark measurements

Ca^{2+} sparks were measured in endothelium-denuded uterine arteries loaded with the Ca^{2+} sensitive dye Fluo-4 AM and using a Zeiss LSM 710 NLO laser scanning confocal imaging workstation on an inverted microscope platform (Zeiss Axio Observer Z1).[30] The endothelium was mechanically disrupted by gently pulling a silver wire across the intimal surface of the uterine arterial segments five times, with confirmation by visual analysis of the preparations on the confocal microscope after loading the tissue with Fluo-4. Arterial segments were incubated with 10 μmol/L Fluo-4 AM (Thermo Fisher, Waltham, MA, USA) dissolved in DMSO along with 0.1% pluronic F127 (Thermo Fisher) for 1–1.5 h at room temperature. Tissues were then washed for 30 min to allow dye esterification and then cut into linear strips. The arterial segments were pinned to Sylgard blocks and placed in an open bath imaging chamber mounted on the confocal imaging stage. Cells were illuminated at 488 nm with a krypton argon laser, and the emitted light was collected using a photomultiplier tube. Line scans were imaged at 529 frames/s with the emission signal recorded at 493–622 nm. The acquisition period for Ca^{2+} spark recordings was 18.9 s. The resultant pixel size ranged from 0.021 to 0.1 μm per pixel. To ensure that sparks within the cell were imaged, the pinhole was adjusted to provide an imaging depth of 2.5 μm. This depth is roughly equivalent to the width of 50% of the cell based on the morphological examination of live preparations. Line scans were analysed using Sparklab 4.2.1 to characterize Ca^{2+} spark parameters such as frequency (sparks/μm/s), amplitude (F/F_0), spatial size [the full width at half maximum (FWHM)], and duration [the full duration at half maximum (FDHM)]. The fractional fluorescence intensity was calculated as $F/F_0 = F$-baseline/F_0-baseline, where baseline is the intensity from a region of interest with no cells, F is the fluorescence intensity for the region of interest, and F_0 is the fluorescence intensity during a period from the beginning of the recording when there was no Ca^{2+} activity.

2.5 Measurement of STOCs

Vascular smooth muscle cells were enzymatically dissociated from resistance-sized uterine arteries as described previously.[15] Briefly, uterine arteries were minced and incubated (37°C, 10 min) in low-Ca^{2+} HEPES-buffered physiological salt (PSS) solution containing (in mmol/L) 140.0 NaCl, 5.0 KCl, 0.1 $CaCl_2$, 1.2 $MgCl_2$, 10.0 HEPES, and 10.0 glucose (pH 7.4). Vessels were then exposed to a two-step digestion process that involved: (i) a 60-min incubation in low-Ca^{2+} HEPES-buffered PSS (37°C) containing 1.5 mg/mL papain (Worthington Biochemical; Lakewood, NJ, USA), 1.5 mg/mL dithiothreitol (MilliporeSigma, St. Louis, MO, USA), and 1.5 mg/mL bovine serum albumin (MilliporeSigma); and (ii) a 60-min incubation in low-Ca^{2+} HEPES-buffered PSS (37°C) containing 1.5 mg/mL collagenase IV (Worthington), and 1.5 mg/mL bovine serum albumin (MilliporeSigma). Following the enzyme treatment, tissues were washed with low Ca^{2+} HEPES-buffered PSS. Single smooth muscle cells were released by gently inverting the tube(s) containing low Ca^{2+} HEPES-buffered PSS and digested tissues several times. The cells were kept at 4°C, and experiments were conducted within 6 h of cell isolation. STOCs were recorded in the whole-cell configuration of the perforated patch-clamp technique using an EPC 10 patch-clamp amplifier with Patchmaster software (HEKA, Lambrecht/Pfalz, Germany) at room temperature as described previously.[15] Briefly, cell suspension drops were placed in a recording chamber, and adherent cells were

continuously superfused with HEPES-buffered PSS containing (in mmol/L) 140.0 NaCl, 5.0 KCl, 1.8 $CaCl_2$, 1.2 $MgCl_2$, 10.0 HEPES, and 10.0 glucose (pH 7.4). Only relaxed and spindle-shaped vascular smooth muscle cells were used for recording. Micropipettes were pulled from borosilicate glass and had resistances of 2–5 MΩ when filled with the pipette solution containing (in mmol/L) 140.0 KCl, 1.0 $MgCl_2$, 5.0 Na_2ATP, 5.0 EGTA, 10.0 HEPES (pH 7.2) with 250 μg/mL amphotericin B. $CaCl_2$ was added to bring free Ca^{2+} concentrations to 100 nmol/L as determined using WinMAXC software (Chris Patton, Stanford University). Membrane currents were recorded while the cells were held at steady membrane potentials between -50 and 10 mV in 10 mV-increments. STOCs were analysed with Mini Analysis program (Synaptosoft, Leonia, NJ, USA) with a threshold for detection set at 10 pA. The currents were normalized to cell capacitance and expressed as picoampere per picofarad (pA/pF).

2.6 Measurement of pressure-dependent myogenic tone

The pressure-dependent myogenic tone of resistance-sized uterine arteries was measured as described previously.[5] Briefly, the arterial segments (~150 μm diameter) were mounted and pressurized in an organ chamber (Living Systems Instruments, Burlington, VT, USA). The intraluminal pressure was controlled by a servo-system to set transmural pressures, and arterial diameter was recorded using the SoftEdge Acquisition Subsystem (IonOptix LLC, Milton, MA, USA). After the equilibration period, the intraluminal pressure was increased in a stepwise manner from 10 to 100 mmHg in 10-mmHg increments, and each pressure was maintained for 5 min to allow vessel diameter to stabilize before the measurement. Ca^{2+}-free PSS contains zero Ca^{2+} and 3 mM EGTA. PSS was allowed to pass through the lumen of the pressurized vessels before the detection of myogenic tone, and the myogenic tone was measured under the static flow. The passive pressure–diameter relationship was conducted in Ca^{2+}-free PSS to determine the maximum passive diameter. The following formula was used to calculate the percentage of pressure-dependent tone at each pressure step: % tone = (D1 - D2)/D1 × 100, where D1 is the passive diameter in Ca^{2+}-free PSS, and D2 is the active diameter with normal PSS in the presence of extracellular Ca^{2+}.

2.7 Immunofluorescence staining and Duolink proximity ligation assay

The co-localization of RyRs and BK_{Ca} channel was examined using immunofluorescent staining as described previously with modifications.[31] After immersion in optimal cutting temperature compound, uterine arteries were sectioned at a thickness of 8 μm using a Leica cryostat (Leica, Buffalo Grove, IL, USA). Uterine arterial slices were blocked in 5% donkey serum (Jackson ImmunoResearch, West Grove, PA, USA) at room temperature (RT) for 1 h, and then incubated with primary antibodies, rabbit polyclonal MaxiKβ antibody (1:200; sc-33608, Santa Cruz Biotechnology), rabbit polyclonal RyR1 antibody (1:100; 8153, Cell Signaling, Danvers, MA, USA), rabbit polyclonal RyR2 (1:100; ARR-002, Alomone Labs, Israel), rabbit polyclonal RyR3 (1:100; AB9082, EMD Millipore), mouse monoclonal BK_{Ca} channel α (1:200; sc-374142), or mouse monoclonal BK_{Ca} channel β1 (1:200; sc-377023) (Santa Cruz Biotechnology, Dallas, TX, USA) at 4°C overnight. After washing with phosphate-buffered saline (PBS), sections were incubated with corresponding fluorescent secondary antibodies (1:1000, Thermo Fisher Scientific) at RT for 1 h, and then mounted and coverslipped using fluorescent mounting media with a classic nuclear counterstain DAPI (diamidino-2-phenylindole) (VECTOR LABORATORIES, INC., Burlingame, CA, USA). All slices were scanned with a Zeiss LSM 710 confocal microscopy (Zeiss, Oberkochen, Germany). Images were acquired using a z-stack of 1.0 μm intervals. Image stacks were analysed using NIH Image J software.

Proximity ligation assay (PLA) was performed using the Duolink in situ kit (MilliporeSigma, St. Louis, MO, USA) according to the manufacturer's instructions. After pre-incubation with a blocking agent for 60 min, cryo-fixed samples were incubated overnight with the primary antibodies against RyR1 or RyR2 (1:300) and BK_{Ca} β1 (1:300). The PLUS and MINUS PLA probes were diluted (1:5 in the Duolink® Antibody Diluent) and applied to the slides, followed by incubation for 2 h in a pre-heated humidity chamber at 37°C. Unbound PLA probes were removed by washing. The samples were incubated in the ligation solution consisting of Duolink Ligation stock (1:5) and Duolink Ligase (1:40) for 30 min at 37°C. Detection of the amplified probe was done with the Duolink Detection Kit. Duolink Detection stock was diluted at 1:5 and applied for 100 min at 37°C. After final washing, coverslips were mounted onto the slides using a minimal volume of Duolink® in situ mounting medium containing DAPI nuclear stain. Image acquisition was carried out on a Zeiss LSM 710 confocal microscopy. Maximum projection images were analysed using ImageJ (National Institutes of Health, Bethesda, MD, USA) to quantify PLA punctate signals. Images were smoothed, and a threshold to distinguish signal from background fluorescence was applied equally to all images and the number of puncta quantified using the 'Analyze Particles' macro with the exclusion criteria of the size of objects being higher than 5 μm.[32]

2.8 Co-immunoprecipitation

The co-immunoprecipitation experiments were performed with Pierce™ Co-Immunoprecipitation Kit (Thermo Fisher Scientific, Waltham, MA, USA) according to the manufacturer's protocol. Briefly, 20 μg of the monoclonal BK_{Ca} α antibody (Santa Cruz Biotechnology, Dallas, TX, USA) were incubated with the delivered resin and covalently coupled. The antibody-coupled resin was incubated with 200 μL of the whole sheep uterine artery protein lysates overnight at 4°C. The resin was washed, and the protein complexes bound to the antibody were eluted. Subsequently, western blot analyses were performed. BK_{Ca} α and BK_{Ca} β1 protein levels in the immunoprecipitates were analysed by monoclonal mouse antibodies against BK_{Ca} α and BK_{Ca} β1 (Santa Cruz Biotechnology) and immunoblotting.

2.9 Statistical analysis

Data were expressed as means ± SEM obtained from the number of experimental animals. Data were analysed with GraphPad Prism (GraphPad Software, San Diego, CA, USA). Differences were evaluated for statistical significance ($P < 0.05$) by one-way analysis of variance (ANOVA) with the *post hoc* Bonferroni/Dunn test or independent-samples *t*-test where appropriate.

3. Results

3.1 Pregnancy increased the co-localization of RyR1 and RyR2 with BK_{Ca} β1 in uterine arteries

BK_{Ca} β1 is the primary sensor of the BK_{Ca} channel to Ca^{2+} sparks mediated by RyRs.[33] Hence, we first determined the spatial organization of BK_{Ca} β1 and RyRs in uterine arteries using immunofluorescence and confocal microscopy. *Figure 1* shows immunofluorescence confocal

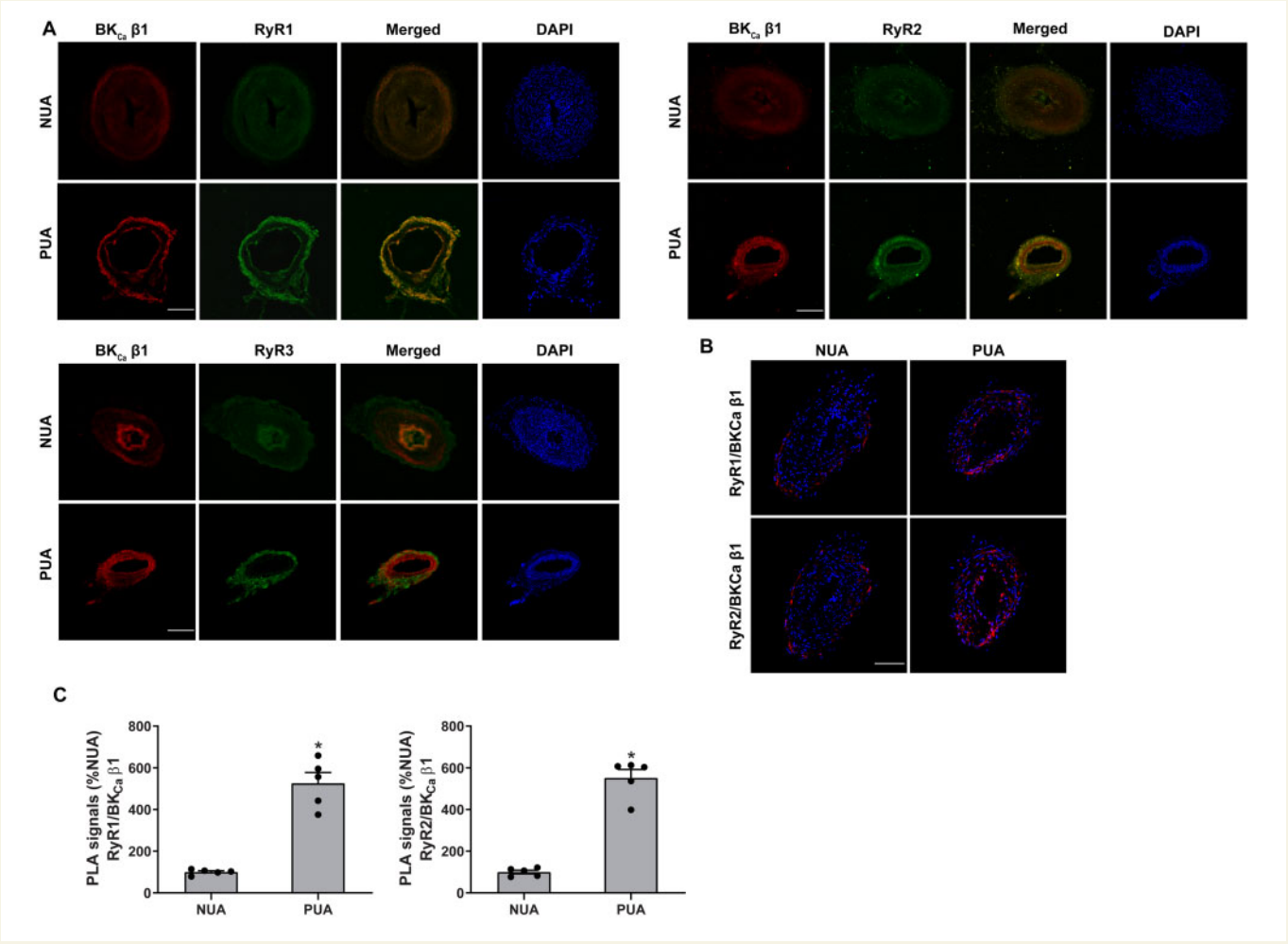

Figure 1 Pregnancy increased co-localization of RyR1/RyR2 with BKCa channel in uterine arteries. (*A*) Representative confocal immunofluorescence images from five replicates show the co-localization of RyRs and BK_{Ca} channels in uterine arteries. Uterine arteries of non-pregnant (NUA) and pregnant (PUA) animals were stained with antibodies against the β1 subunit of BK_{Ca} channel (BK_{Ca} β1, red) and RyR1, RyR2, or RyR3 (green). Merged images show the co-localization of RyR1 or RyR2 with BK_{Ca} β1 (in yellow). The nuclear region was stained with DAPI and shows in blue. Scale bar: 100 μm. (*B*) PLA assay to confirm the co-localization of RyR1/RyR2 and BK_{Ca} β1 in uterine arteries. (*C*) Quantification of the PLA signals. Images from five independent replicates were analysed. The nuclear region was stained with DAPI and shown in blue. Scale bar: 50 μm. Data are means ± SEM from five animals of each group; independent-samples *t*-test; $^*P < 0.05$, PUA vs. NUA.

images of BK_{Ca} β1 and RyRs expression in uterine arteries of non-pregnant and pregnant sheep. Apparently, pregnancy increased the expression of BK_{Ca} β1 and all three subtypes of RyRs in the tunica media of uterine arteries (*Figure 1A*), consistent with western blot findings in our previous studies.[5,15] Moreover, pregnancy also promoted immunofluorescence co-localization of BK_{Ca} β1 with RyR1 and RyR2, respectively. In contrast, the co-localization of BK_{Ca} β1 with RyR3 was negligible and not affected by pregnancy. The interactions between BK_{Ca} β1 and RyR1/RyR2 were further examined using the PLA assay. As shown in *Figures* 1B *and C*, pregnancy significantly increased the close co-localization between BK_{Ca} β1 and RyR1/RyR2.

3.2 Knockdown of RyRs functionally impaired Ca^{2+} sparks and STOCs in uterine arteries

Our previous study revealed that pan-inhibition of RyRs with ryanodine inhibited the Ca^{2+} spark-STOC coupling in uterine arteries of pregnant sheep.[15] To determine the functional importance of individual RyR subtypes, we examined Ca^{2+} sparks and STOCs in uterine artery vascular smooth muscle cells following knockdown of each RyR subtype using siRNAs. As shown in Supplementary material online, *Figure S1*, the expression levels of mRNA and protein of each RyR1, RyR2, and RyR3 in uterine arteries were significantly reduced by corresponding RyR siRNAs. *Figure 2A* illustrates representative line-scan confocal images of Ca^{2+} sparks in control siRNA and RyR siRNA-treated uterine arteries from pregnant sheep loaded with the Ca^{2+} indicator Fluo-4. The percentage of Ca^{2+} spark firing smooth muscle cells in uterine arteries was not significantly altered by the knockdown of RyRs (*Figure 2B*). However, the ability of membrane depolarization with 30 mmol/L K^+ to stimulate Ca^{2+} spark frequency was significantly decreased by the knockdown of RyR1 and RyR2, respectively, but not significantly affected by RyR3 knockdown (*Figure 2C*). The other Ca^{2+} spark parameters such as amplitude (F/F_0), width (FWHM), and duration (FDHM) were not or slightly altered by knocking down RyRs in uterine arterial smooth muscle cells (Supplementary material online, *Figure S2*).

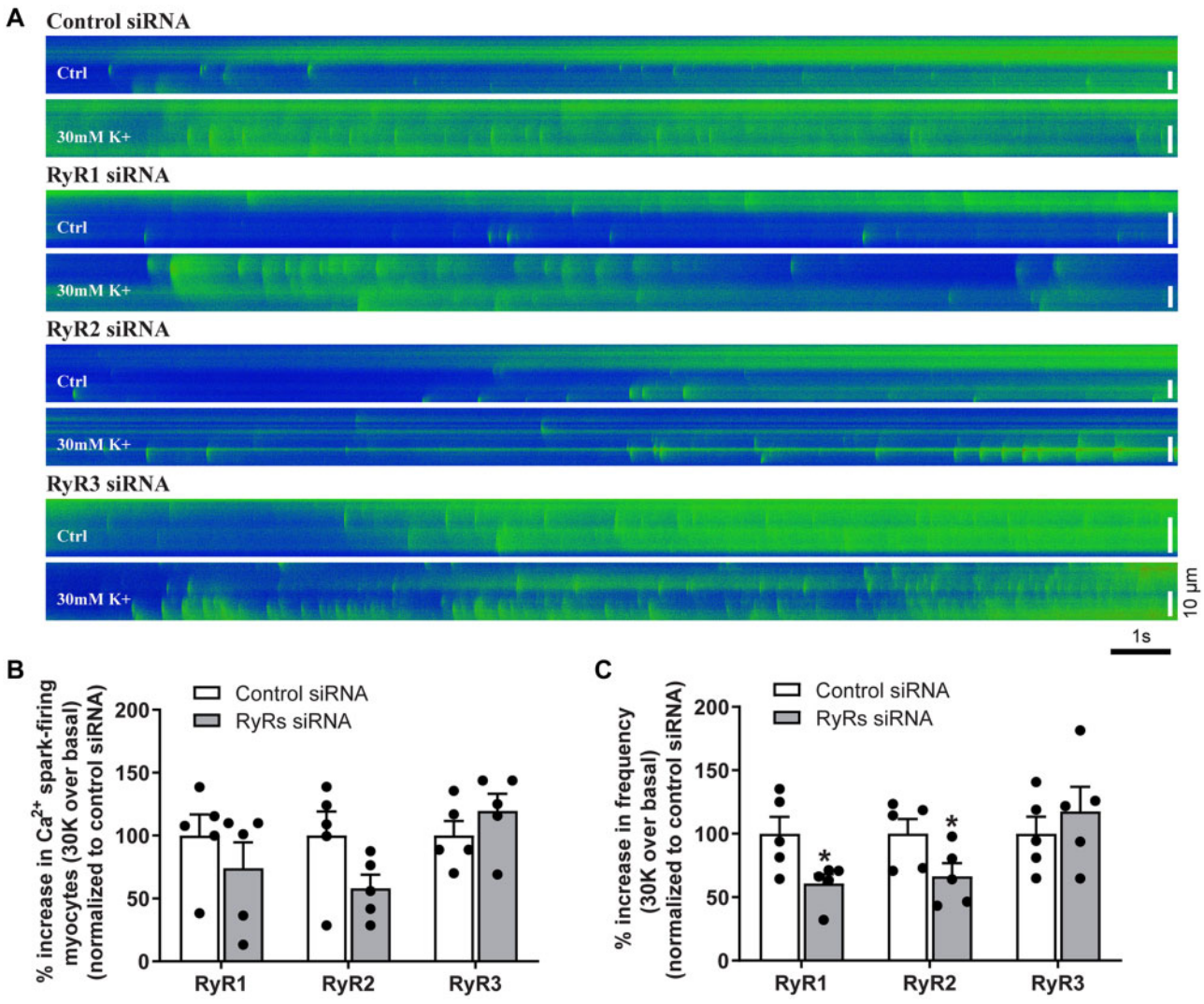

Figure 2 Knockdown of RyR1/RyR2 decreased Ca^{2+} sparks in uterine arteries of pregnant sheep. Uterine arteries of pregnant animals were treated with scramble control siRNA or siRNAs for RyR1, RyR2, and RyR3, respectively. Ca^{2+} sparks in uterine arteries were measured 48 h later. (*A*) Representative line-scan images of Fluo-4AM loaded uterine arteries showing Ca^{2+} sparks recorded before and after the sequential application of 30 mmol/L K^+ (30 K) following siRNA treatments. (*B*) Percentage of Ca^{2+} spark-firing vascular smooth muscle cells. (*C*) Ca^{2+} spark frequency. Data are means ± SEM from five animals of each group; independent-samples *t*-test; *$P < 0.05$, RyR siRNAs vs. control siRNA.

We then examined the contribution of individual RyRs in the regulation of STOCs in uterine arteries of pregnant sheep. *Figure 3A* shows representative tracing of STOCs in vascular smooth muscle cells isolated from uterine arteries treated with either scramble control siRNA or RyR siRNAs at a holding potential of 10 mV. In agreement with the actions of RyR siRNAs on Ca^{2+} sparks, RyR1 and RyR2, but not RyR3, knockdown suppressed STOCs. The occurrence of STOCs in RyR1/RyR2-knockdown uterine artery vascular smooth muscle cells was shifted to a much more positive membrane potential (from -40 mV to -20 mV), approximating the phenotype of non-pregnant animals, as demonstrated previously.[15] Moreover, knockdown of RyR1 or RyR2 significantly reduced both STOC frequency (*Figure 3B*) and amplitude (*Figure 3C*) at membrane potentials between -30 and 10 mV. For example, STOC frequency and amplitude at 10 mV were decreased by 44.7 ± 5.5% and 60.1 ± 4.4% in RyR1-knockdown uterine artery vascular smooth muscle cells, and by 57.2 ± 1.7% and 71.2 ± 2.3% in RyR2-knockdown uterine artery vascular smooth muscle cells, respectively. In contrast, RyR3 knockdown did not significantly alter STOC frequency and amplitude (*Figure 3B and C*). Treatments with control siRNA or RyR siRNAs apparently did not alter the inhibitory effect of BK_{Ca} channel inhibitor iberiotoxin on STOCs. Similar to the previous findings in vascular smooth muscle cells from freshly harvested uterine arteries,[15] iberiotoxin produced a progressive inhibition of STOCs in smooth muscle cells of siRNA-treated uterine arteries (Supplementary material online, *Figure S3*).

3.3 Ryr1 and RyR2 knockdown increased pressure-dependent myogenic tone in uterine arteries

Increased Ca^{2+} sparks and STOCs are of critical importance in pregnancy-induced attenuation in uterine arterial myogenic tone.[15]

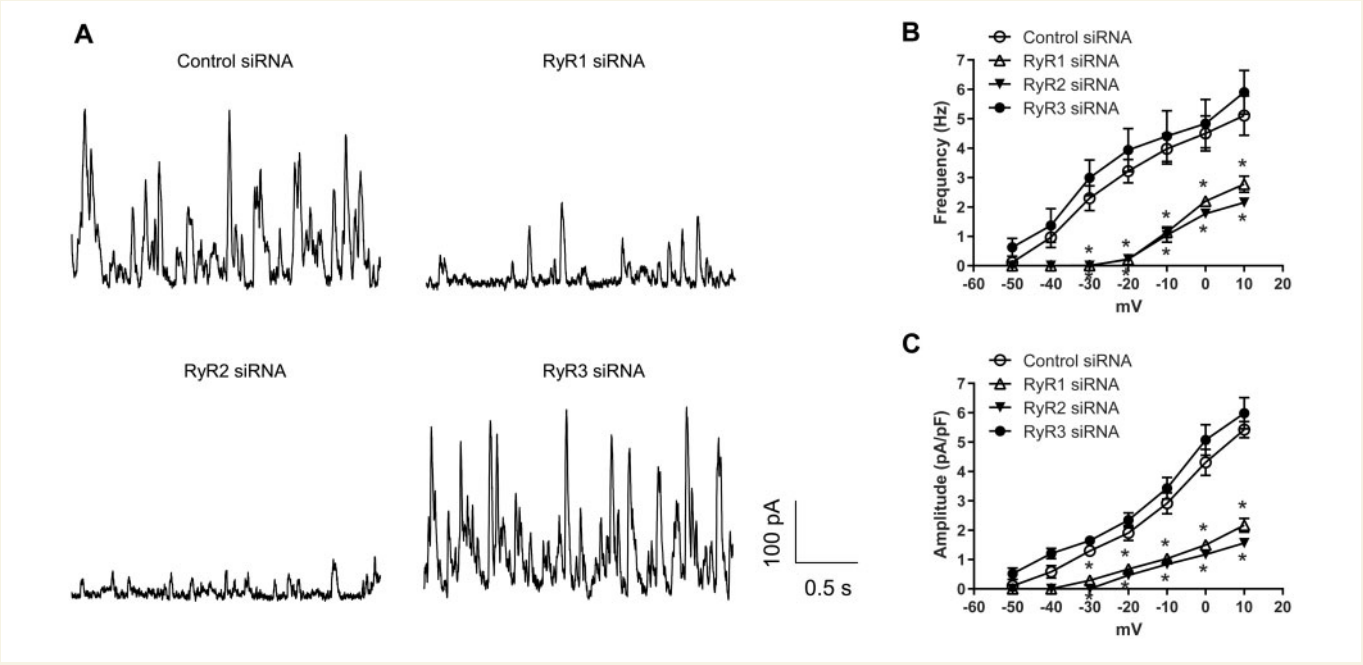

Figure 3 Knockdown of RyR1/RyR2 suppressed STOCs in uterine arteries of pregnant sheep. Uterine arteries of pregnant animals were treated with scramble control siRNAs or siRNAs for RyR1, RyR2, and RyR3, respectively. STOCs were measured in uterine artery vascular smooth muscle cells 48 hours later. (*A*) Representative traces showing STOCs at holding potentials of 10 mV in uterine artery vascular smooth muscle cells. (*B*) STOC frequency. (*C*) STOC amplitude. Data are means ± SEM from five animals of each group; repeated measures ANOVA with the *post hoc* Bonferroni/Dunn test; *$P < 0.05$, RyR siRNAs vs. control siRNA.

We thus investigated the functional importance of individual RyR subtypes in regulating pressure-dependent myogenic tone in uterine arteries of pregnant animals by knocking down individual RyR subtypes. Representative traces and averaged data of the myogenic response were shown in Supplementary material online, *Figure S4* and *Figure 4A–C*, respectively. As shown in *Figure 4*, knockdown of RyR1 or RyR2 significantly increased pressure-dependent myogenic tone (*Figure 4D*). Consistent with the lack of effect on Ca^{2+} sparks and STOCs, knockdown of RyR3 had no significant effect on uterine arterial myogenic tone (*Figure 4D*). Control siRNA had no effect on myogenic tone compared to the untreated control (*Figure 4D*). Furthermore, treatment with control siRNA did not alter the effect of iberiotoxin on increasing uterine arterial myogenic tone (Supplementary material online, *Figure S5*). Our previous study demonstrated that iberiotoxin or RyR blockade with ryanodine increased myogenic tone of uterine arteries from pregnant sheep, and combined action of iberiotoxin and ryanodine did not produce additive effects on myogenic tone, as compared to the response induced by each alone.[15] Similar findings were obtained in the present study. Iberiotoxin had no additive effect on increased myogenic tone induced by knockdown of RyR1 or RyR2, respectively (Supplementary material online, *Figure S5*). In contrast to pregnant animals, treatments of uterine arteries of non-pregnant animals with RyR siRNAs had no significant effect on myogenic tone (Supplementary material online, *Figure S6*).

3.4 Ryrs regulated BK_{Ca} β1 expression and its association to BK_{Ca} α subunit in uterine arteries

The BK_{Ca} channel in smooth muscle cells is heteromeric of the pore-forming α subunit and auxiliary β1 subunit.[34,35] The β1:α subunit stoichiometry is dynamically regulated under various physiological and pathophysiological conditions and plays a vital role in regulating the BK_{Ca} channel activity in vascular smooth muscle. As shown in *Figure 5A*, co-immunoprecipitation and western blot demonstrated that pregnancy increased the association of BK_{Ca} α and BK_{Ca} β1 in uterine arteries. Co-localization of BK_{Ca} α and BK_{Ca} β1 examined by immunofluorescence confocal microscopy revealed that knockdown of RyR1 or RyR2, but not RyR3, decreased the co-localization of BK_{Ca} α and BK_{Ca} β1 (*Figure 5B*). This was further confirmed by co-immunoprecipitation and western blot, as illustrated in *Figure 5C*. Of interest, knockdown of either RyR1 or RyR2 in uterine arteries of pregnant sheep markedly reduced protein abundance of BK_{Ca} β1 when compared to the scramble control siRNA treatment (*Figure 6A and B*). In contrast, the protein expression of BK_{Ca} α was not altered by RyR1/RyR2 knockdown (*Figure 6A and B*). Unlike RyR1 or RyR2, RyR3 knockdown altered neither BK_{Ca} α nor BK_{Ca} β1 protein expression (*Figure 6C*).

4. Discussion

In the present study, we examined the contribution of individual RyR subtypes to pregnancy-induced increase in the Ca^{2+} spark-STOC coupling and uterine vascular adaptation. The major findings are: (i) pregnancy increased the co-localization of BK_{Ca} β1 and RyR1/RyR2 in uterine arteries; (ii) RyR3 was not co-localized with BK_{Ca} β1; (iii) RyR1 or RyR2, but not RyR3, knockdown impaired Ca^{2+} sparks/STOCs and increased myogenic tone in uterine arteries; (iv) pregnancy augmented the association of BK_{Ca} α and BK_{Ca} β1 in uterine arteries, which was suppressed by RyR1/RyR2, but not RyR3, knockdown; (v) knockdown of

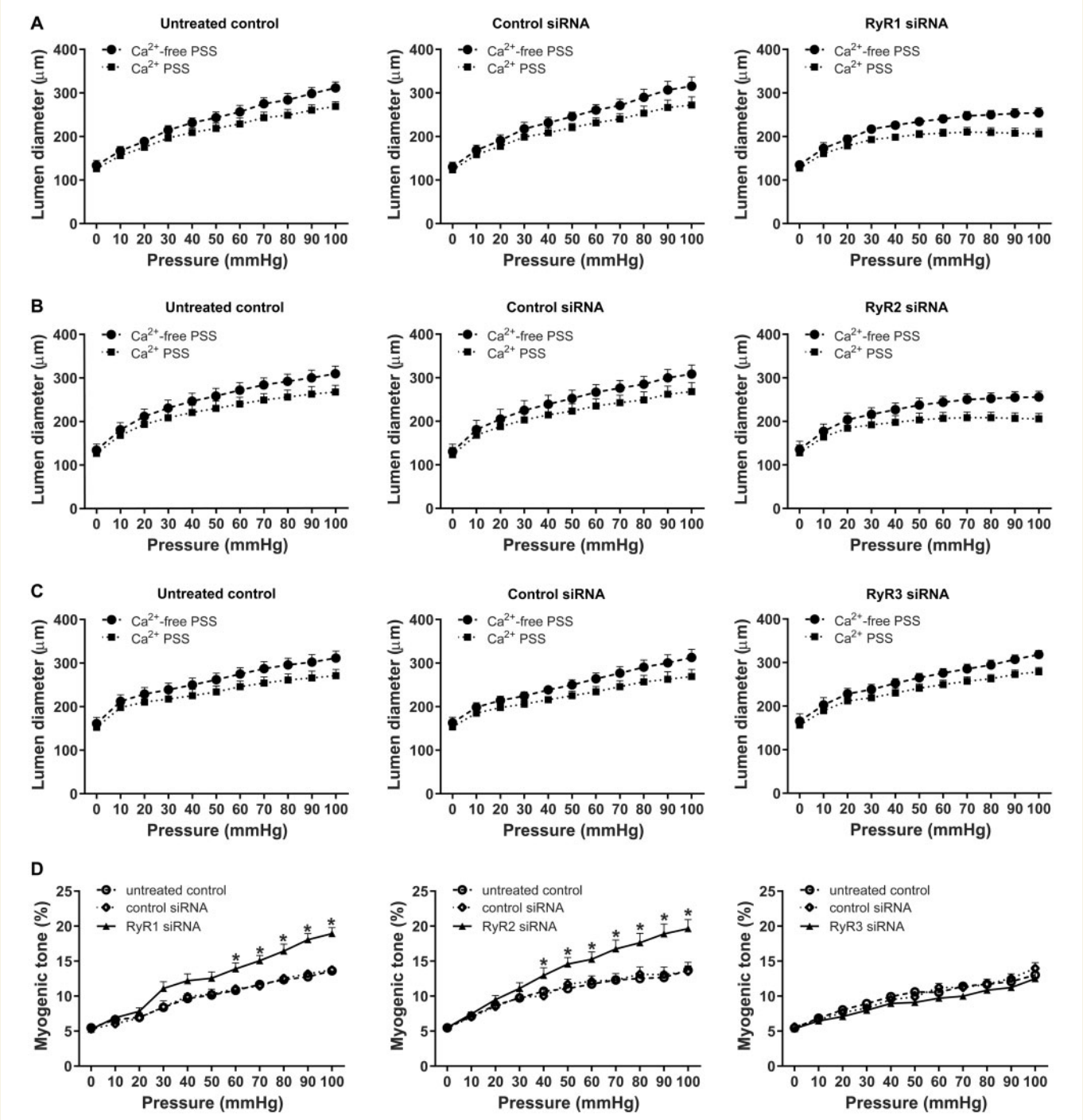

Figure 4 Knockdown of RyR1/RyR2 increased myogenic tone in uterine arteries of pregnant sheep. Uterine arteries of pregnant animals were treated with scramble control siRNAs or siRNAs for RyR1, RyR2, and RyR3, respectively. Pressure-dependent myogenic tone was measured in uterine arteries 48 h later. (*A–C*) Changes of lumen diameters of uterine arteries in response to increases in intravascular pressure. (*D*) Data summary showing the percentage myogenic tone in RyR siRNA-treated uterine arteries. Data are means ± SEM from five animals of each group; repeated measures ANOVA with the post hoc Bonferroni/Dunn test; $^*P < 0.05$, RyR siRNAs vs. untreated control or control siRNA.

RyR1/RyR2 deceased BK_{Ca} β1 but not BK_{Ca} α expression in uterine arteries.

Owing to its large conductance and high density, the BK_{Ca} channel plays a critical role in regulating vascular smooth muscle cell membrane potential and vascular tone.[36] Although the BK_{Ca} channel can be activated by either voltage or Ca^{2+}, its activity in smooth muscle cells is primarily regulated by Ca^{2+} sparks mediated by RyRs under physiological conditions.[37] The binding affinity (Kd) of Ca^{2+} for the BK_{Ca} channel in smooth muscle cells is ~20 μmol/L at the physiological membrane potential around -40 mV. A single Ca^{2+} sparks can rise $[Ca^{2+}]_i$ to 10–

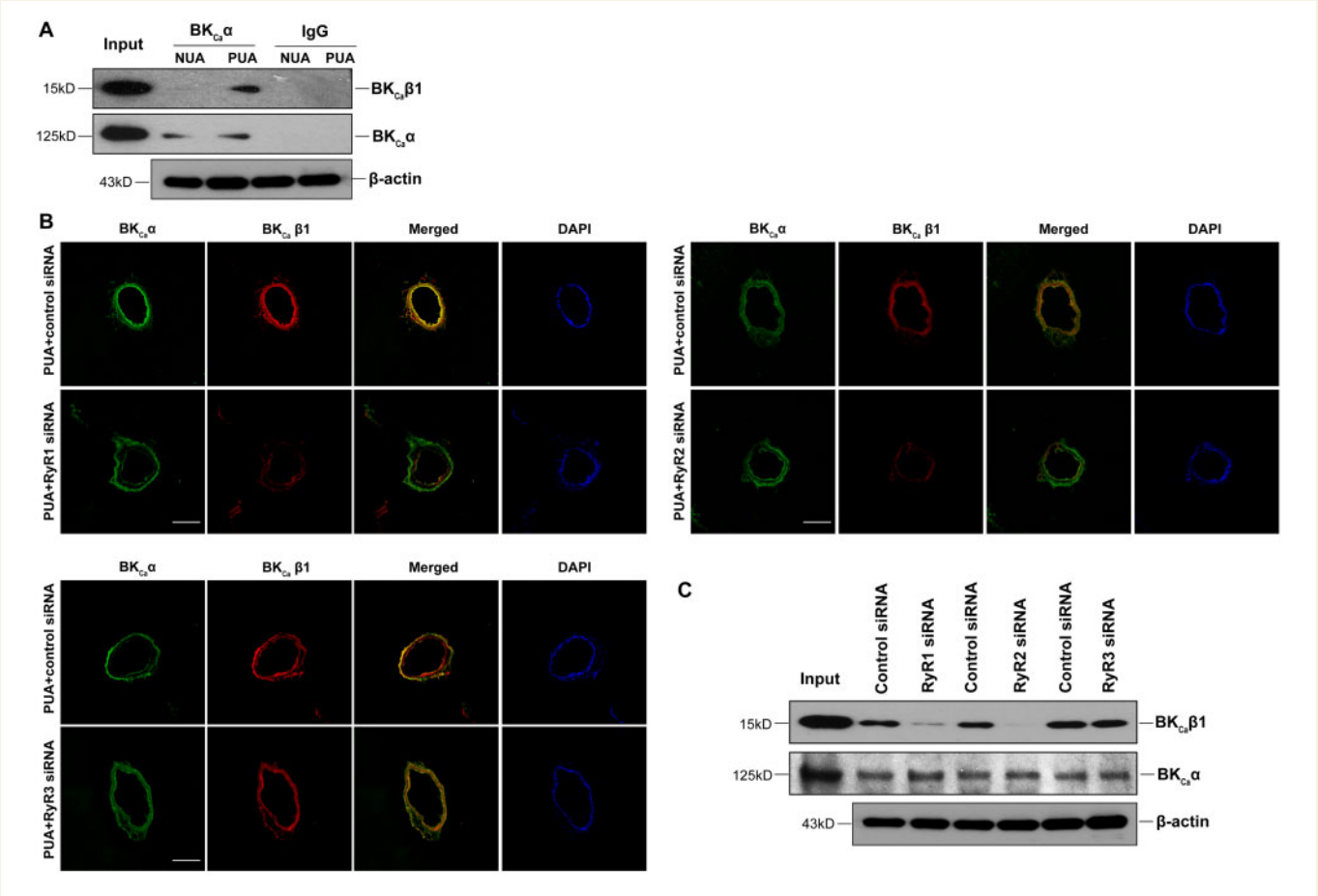

Figure 5 Knockdown of RyR1/RyR2 reduced the interaction of BK_{Ca} channel α and β1 subunits in uterine arteries. (*A*) Representative immunoblots from five replicates show co-immunoprecipitation of BK_{Ca} channel α and β1 subunits in uterine arteries of non-pregnant (NUA) and pregnant (PUA) sheep. Uterine arteries were treated with scramble control siRNA or siRNAs for RyR1, RyR2, and RyR3, respectively, for 48 h. IgG was used as a control to show antibody specificity. (*B*) Representative confocal immunofluorescence images from five replicates show the co-localization of BK_{Ca} channel α and β1 subunits in uterine arteries of pregnant sheep after control siRNAs or RyR siRNAs treatments. The arteries were stained with antibodies against α (green) and β1 (red) subunits. Merged images show in yellow. The nuclear region was stained with DAPI and shows in blue. Scale bar: 100 μm. (*C*) Representative immunoblots from five replicates show co-immunoprecipitation of BK_{Ca} channel α and β1 subunits in uterine arteries of pregnant sheep after control siRNA or RyR siRNAs treatments. β-Actin blots showing equal total protein lysates (input).

30 μmol/L, and this Ca^{2+} microdomain covers a radius of ~200 nm.[22,38] It should be noted that $[Ca^{2+}]_i$ decreases sharply when it travels away from the Ca^{2+} source.[21,25] This requires proper spatial organization of the BK_{Ca} channel and RyRs for the BK_{Ca} channel to sense the Ca^{2+} signal within the Ca^{2+} microdomain. The BK_{Ca} channel is a heteromeric assembly of the pore-forming BK_{Ca} α and auxiliary BK_{Ca} β1 in smooth muscle cells and the association of BK_{Ca} β1 to BK_{Ca} α significantly increases the channel activity by enhancing channel's Ca^{2+} sensitivity.[33,39] BK_{Ca} α co-localized with RyR1/RyR2 in airway and cerebral arterial vascular smooth muscle cells.[25,40] To our knowledge, the present study is the first to show the co-localization of BK_{Ca} β1 and RyR1/RyR2 in uterine artery vascular smooth muscle cells using immunofluorescence and confocal microscopy and proximity ligation assay that detects protein–protein interaction within 40 nm. It remains to be determined whether the co-localization of RyRs with BK_{Ca} β1 may alter the association between BK_{Ca}α and BK_{Ca}β1 subunits. Similar to the dynamic association of BK_{Ca} β1 and BK_{Ca} α subunits in vascular smooth muscle cells,[41] it is likely that the co-localization of BK_{Ca} β1 with RyR1/RyR2 in uterine artery vascular smooth muscle cells also undergoes a dynamic process. It is currently not known whether the co-localization of RyR1/RyR2 with BK_{Ca} β1 may alter the half-life of BK_{Ca} β1. Such a spatial proximity keeps BK_{Ca} β1 in close contact with RyRs and enables BK_{Ca} channel to be activated by Ca^{2+} sparks, facilitating the functional coupling between Ca^{2+} sparks and STOCs. A disruption of this spatial organization may impair the coupling. For example, an increase in the distance between sarcoplasmic reticulum and plasma membranes by microtubule depolymerization using nocodazole reduced the number of close contacts between BK_{Ca} α and RyR2 in rat cerebral arteries, leading to almost abolition of STOCs.[26] Whether and to what extent SR distance from the plasma membrane is altered during pregnancy remain to be determined. Only a small fraction of BK_{Ca} channels and RyRs are co-localized in smooth muscle cells.[25,40] Interestingly, pregnancy significantly increased the co-localization of BK_{Ca} β1 and RyR1/RyR2, suggesting potentially increased contact sites between these proteins, which may account for the

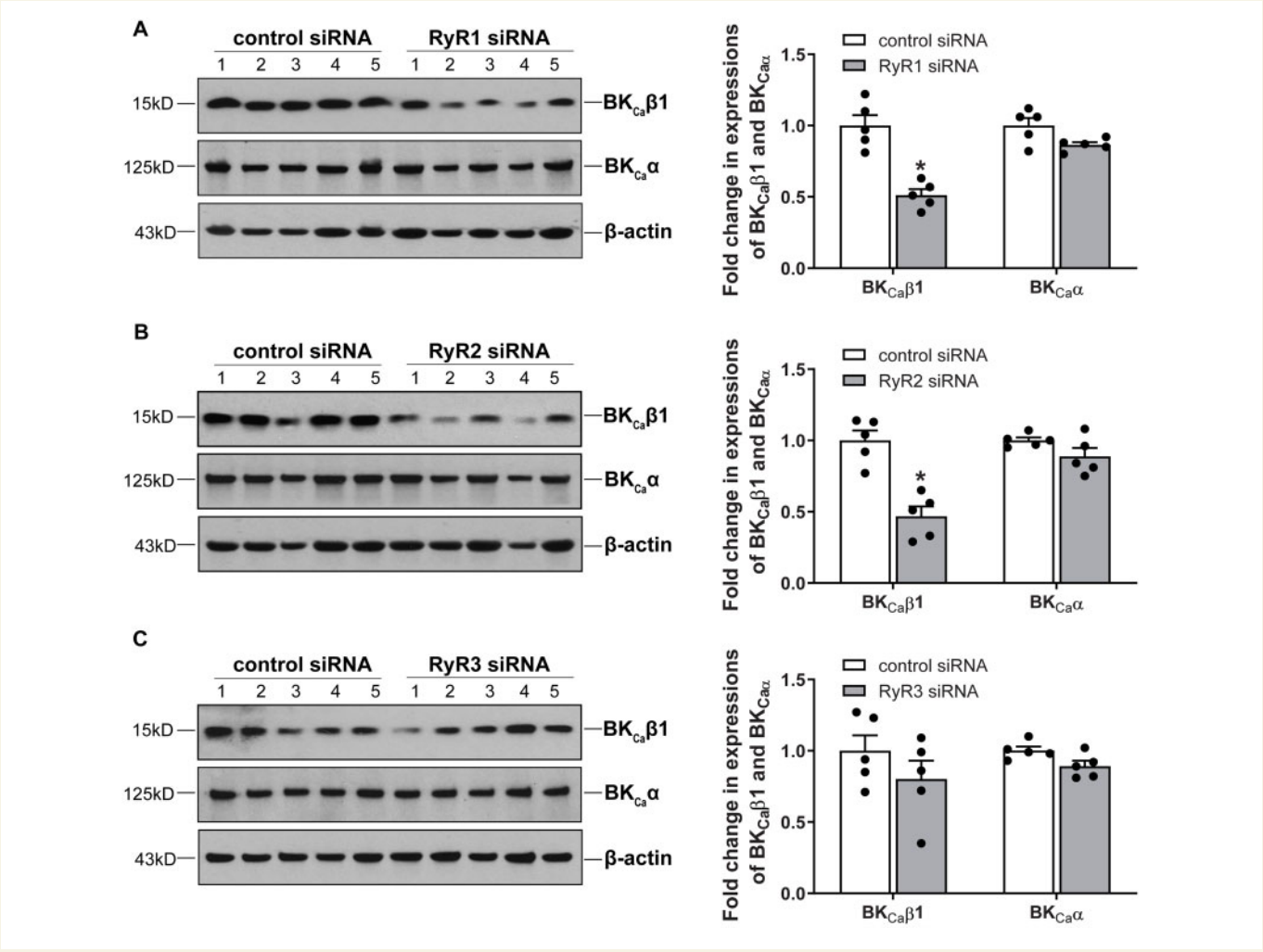

Figure 6 Knockdown of RyR1/RyR2 downregulated the expression of BK_{Ca} channel β1 subunit in uterine arteries of pregnant animals. Uterine arteries of pregnant sheep were treated with scramble control siRNA or siRNAs for RyR1, RyR2, and RyR3, respectively. Protein abundance of BK_{Ca} channel α and β1 subunits was measured by western blot in uterine arteries 48 h after the treatment. (*A*) RyR1 siRNAs treatment. (*B*) RyR2 siRNAs treatment. (*C*) RyR3 siRNAs treatment. Data are means ± SEM from five animals of each group; independent-samples *t*-test; $^*P < 0.05$, RyR siRNAs vs. control siRNA.

enhanced Ca^{2+} spark-STOC coupling in uterine arteries of pregnant animals, as demonstrated in our previous study.[15] Among other mechanisms, the increased co-localization of BK_{Ca} β1 and RyR1/RyR2 is probably due to their upregulation in uterine arteries.[5,15] Previous studies demonstrated that BK_{Ca}β1 and RyR1/RyR2 mRNA and protein levels in uterine arteries increased in a parallel manner during pregnancy,[5,15] suggesting an increase in transcription. It also remains possible that pregnancy may alter half-lives of these proteins, which may contribute to the increase in their abundance in uterine arteries.

The close co-localization of RyRs and BK_{Ca} channels allows BK_{Ca} β1 to function as a vital relay that functionally couples the Ca^{2+} sparks to STOCs. The integrity of the coupling machinery is essential for signal transduction. Knockdown of RyR1/RyR2, which could interrupt the coupling of RyRs and BK_{Ca} channels, impaired the Ca^{2+} spark-STOC coupling as evidenced by blunted 30 mmol/L K^+-stimulated Ca^{2+} spark activity and diminished STOCs in uterine artery vascular smooth muscle cells. These findings are in agreement with previous observations.[17–19,42] The finding that knockdown of RyR1/2 had no significant effect on the proportion of Ca^{2+} spark-firing smooth muscle cells, but reduced Ca^{2+} spark frequency is intriguing and suggests that the primary action of RyR knockdown is to reduce Ca^{2+} spark frequency within the cells (which hence decreases the Ca^{2+} spark-STOC coupling), but not the number of firing cells. This is consistent with the notion that gene knockdown only reduces, but not silences, the gene of interest in the cells. In contrast to RyR1/RyR2, RyR3 was not co-localized with BK_{Ca} β1 in uterine arteries. Similarly, RyR3 and BK_{Ca} α were not co-localized in airway smooth muscle cells.[25] Functionally, RyR3 knockdown did not alter either Ca^{2+} sparks or STOCs. This is in line with observations reported by Mironneau *et al.*,[17] but not by Löhn *et al.* and Matsuki *et al.*[20,43] The finding that RyR1/RyR2, but not RyR3 was co-localized with BK_{Ca} β1 is intriguing. Several previous studies demonstrated a distinct spatial distribution of RyRs in smooth muscle cells.[25,44–46] In general, RyR2 is predominantly located in the subplasmalemmal region and RyR3 is in the perinuclear region, whereas RyR1 is located in both subplasmalemmal and perinuclear regions. This distinct spatial distribution of RyRs is likely to contribute to the differential interaction of RyRs and BK_{Ca} channels.

The aberrant expression of BK_{Ca} β1 could also impact the Ca^{2+} spark-STOC coupling in vascular smooth muscle cells. The coupling was attenuated and boosted by BK_{Ca} β1 deficiency and BK_{Ca} β1 overexpression, respectively.[23,33,47]

We previously demonstrated that enhanced Ca^{2+} spark-STOC coupling in the uterine arteries during pregnancy was associated with upregulation of all three subtypes of RyRs.[15] Physiologically, the enhanced Ca^{2+} spark-STOC coupling during pregnancy was found to promote uterine vascular adaptation by attenuating uterine arterial myogenic tone.[15] However, the roles of individual RyRs in the pregnancy-induced enhancement of Ca^{2+} spark-STOC coupling remain elusive. Interestingly, in the present study, we demonstrated that knockdown of RyR1/RyR2, but not RyR3, in uterine arteries of pregnant animals repressed the Ca^{2+} spark-STOC coupling and increased uterine arterial myogenic tone. The finding that knockdown of RyR1/2 has little effect on myogenic tone in uterine arteries of non-pregnant animals is not surprising, and indeed is consistent with the previous finding that the pan-inhibition of ryanodine receptors with ryanodine had no significant effect on myogenic tone in uterine artery of non-pregnant sheep.[15] Apparently, repressing RyR1/RyR2 in uterine arteries of pregnant animals using the RNA interference tool produced a phenotype resembles uterine arteries of non-pregnant animals. The finding that siRNAs knockdown RyR1 and RyR2 about 40% at the mRNA level but about 60% of protein abundance is not surprising. Indeed, it is not uncommon that changes in mRNA abundance may not always precisely correlate to changes in protein abundance due to post-transcriptional, translational, and protein degradation regulations.[48–50] Although downregulation of RyRs had no significant effect on Ca^{2+} spark firing smooth muscle cells, knockdown of RyR1 and RyR2 significantly decreased Ca^{2+} spark frequency, STOC frequency and amplitude, and increased myogenic tone in uterine arteries. Thus, the present study established a cause-and-effect relationship between RyR1/RyR2 and the Ca^{2+} spark-STOC coupling in the regulation of uterine arterial myogenic tone during pregnancy. Although RyR3 is upregulated in uterine arteries during pregnancy,[15] its physiological relevance is currently unclear. Both RyR1 and RyR2 participate in generating Ca^{2+} sparks in smooth muscle cells.[18,19,51] Arterial stiffness is affected by vascular smooth muscle cell tone.[52] It is not surprising that knockdown of RyR1 or RyR2 affected arterial stiffness via altering myogenic tone in uterine arteries. The apparent redundancy of increasing both RyR1 and RyR2 in uterine arteries during pregnancy is likely to provide a protective mechanism to ensure the adaptation of Ca^{2+} dynamics and myogenic tone in uterine arteries and the optimization of uterine blood flow during pregnancy. Whether and to what extent RyR1 and RyR2 may produce additive or synergistic effect in the regulation of Ca^{2+} sparks remains to be determined. Together, this study revealed an explicit contribution of RyR1/RyR2 in mediating enhanced Ca^{2+}-release events that resulted in reduced vascular tone in the uterine circulation during pregnancy.

The association of BK_{Ca} β1 to BK_{Ca} α is essential for the channel to regulate arterial vascular smooth muscle cell membrane potential, contractility, and blood pressure.[23,33,35] It is not surprising that pregnancy increased the association of BK_{Ca} β1 to BK_{Ca} α in the uterine artery in the present study. However, it is somewhat surprising that RyR1/RyR2 knockdown promoted BK_{Ca} β1 downregulation and decreased the association of BK_{Ca} α and BK_{Ca} β1 in uterine arteries of pregnant animals. These observations are puzzling at first glance. However, digging into Ca^{2+} sparks' action could help unfold this mysterious issue. RyR-mediated Ca^{2+} sparks in vascular smooth muscle cells have been shown to counter vasoconstriction via BK_{Ca} channel-mediated hyperpolarization of the vascular smooth muscle cell membrane and closing $Ca_V1.2$.[10,11] It is conceivable that RyR1/RyR2 knockdown would diminish the inhibitory effect of Ca^{2+} sparks on $Ca_V1.2$ in uterine artery vascular smooth muscle cells, thus leading to increased Ca^{2+} influx through $Ca_V1.2$. The regulation of gene expression by $Ca_V1.2$ activity is a well-established phenomenon and frequently involves transcription factors such as cAMP-response element binding protein and nuclear factor of activated T-cells (NFAT).[53] Intriguingly, in an animal model of hypertension, *in vivo* administration of angiotensin II activated NFATc3 via stimulating $Ca_V1.2$-mediated Ca^{2+} influx.[54] The activation of NFATc3 consequently led to downregulation of BK_{Ca} β1 in vascular smooth muscle cells. Significantly, RyR inhibition with ryanodine enhanced transcriptional activities of NFAT in skeletal muscle fibres and potentiated UTP-induced NFATc3 nuclear accumulation in cerebral arteries.[55,56] It is possible that RyR1/RyR2 knockdown induces the activation of NFATc3, which confers the downregulation of BK_{Ca} β1 in uterine arteries. The diminished BK_{Ca}β1 abundance in uterine arterial smooth muscle probably then contributed to the reduced association of BK_{Ca} α and BK_{Ca} β1. To our knowledge, this study is the first to provide evidence that RyR1/RyR2 participate in the regulation of BK_{Ca} β1 expression. These findings suggest that RyRs play an important role in maintaining BK_{Ca} β1 homeostasis and the dynamic interaction of BK_{Ca} α and BK_{Ca} β1 in the uterine artery in pregnancy.

Adequate uterine vascular adaptation is essential for a successful pregnancy. We recently demonstrated an important role of RyR-mediated Ca^{2+} sparks and BK_{Ca} channel-mediated STOCs in this adaptation.[15] In the present study, we revealed (i) enhanced close co-localization between RyR1/RyR2 and BK_{Ca} β1 in uterine arteries during pregnancy and (ii) a cause-and-effect relationship of RyR1/RyR2 in the enhanced Ca^{2+} spark-STOC coupling and attenuated uterine arterial myogenic tone in uterine arteries of pregnant animals. Moreover, our findings also suggest the regulatory divergence of RyRs on the Ca^{2+} spark-STOC cascade at two levels: direct regulation of Ca^{2+} sparks and indirect regulation of BK_{Ca} β1 expression and the dynamic interaction of BK_{Ca} α and BK_{Ca} β1 as a consequence of altered Ca^{2+} sparks. Together, these novel findings provide new mechanistic insights into pregnancy-induced uterine vascular adaptation.

Supplementary material

Supplementary material is available at *Cardiovascular Research* online.

Acknowledgements

A portion of this research used the Loma Linda University School of Medicine Advanced Imaging and Microscopy Core, a facility supported in part by the National Science Foundation through the Major Research Instrumentation program of the Division of Biological Infrastructure Grant No. 0923559 and the Loma Linda University School of Medicine.

Conflict of interest: none declared.

Funding

This work was supported by National Institutes of Health Grants (HD083132, HL128209, and HL137649 to L.Z.).

References

1. Ducsay CA, Goyal R, Pearce WJ, Wilson S, Hu XQ, Zhang L. Gestational hypoxia and developmental plasticity. *Physiol Rev* 2018;**98**:1241–1334.
2. Rosenfeld CR, White RE, Roy T, Cox BE. Calcium-activated potassium channels and nitric oxide coregulate estrogen-induced vasodilation. *Am J Physiol Heart Circ Physiol* 2000;**279**:H319–H328.
3. Rosenfeld CR, Roy T, DeSpain K, Cox BE. Large-conductance Ca2+-dependent K+ channels regulate basal uteroplacental blood flow in ovine pregnancy. *J Soc Gynecol Investig* 2005;**12**:402–408.
4. Rosenfeld CR, Liu XT, DeSpain K. Pregnancy modifies the large conductance Ca2+-activated K+ channel and cGMP-dependent signaling pathway in uterine vascular smooth muscle. *Am J Physiol Heart Circ Physiol* 2009;**296**:H1878–H1887.
5. Hu XQ, Xiao D, Zhu R, Huang X, Yang S, Wilson S, Zhang L. Pregnancy upregulates large-conductance Ca(2+)-activated K(+) channel activity and attenuates myogenic tone in uterine arteries. *Hypertension* 2011;**58**:1132–1139.
6. Hu XQ, Dasgupta C, Chen M, Xiao D, Huang X, Han L, Yang S, Xu Z, Zhang L. Pregnancy reprograms large-conductance Ca(2+)-activated K(+) channel in uterine arteries: roles of ten-eleven translocation methylcytosine dioxygenase 1-mediated active demethylation. *Hypertension* 2017;**69**:1181–1191.
7. Hu XQ, Dasgupta C, Xiao D, Huang X, Yang S, Zhang L. MicroRNA-210 targets ten-eleven translocation methylcytosine dioxygenase 1 and suppresses pregnancy-mediated adaptation of large conductance Ca(2+)-activated K(+) channel expression and function in ovine uterine arteries. *Hypertension* 2017;**70**:601–612.
8. Brayden JE, Nelson MT. Regulation of arterial tone by activation of calcium-dependent potassium channels. *Science* 1992;**256**:532–535.
9. Perez GJ, Bonev AD, Patlak JB, Nelson MT. Functional coupling of ryanodine receptors to KCa channels in smooth muscle cells from rat cerebral arteries. *J Gen Physiol* 1999;**113**:229–238.
10. Nelson MT, Cheng H, Rubart M, Santana LF, Bonev AD, Knot HJ, Lederer WJ. Relaxation of arterial smooth muscle by calcium sparks. *Science* 1995;**270**:633–637.
11. Knot HJ, Standen NB, Nelson MT. Ryanodine receptors regulate arterial diameter and wall [Ca2+] in cerebral arteries of rat via Ca2+-dependent K+ channels. *J Physiol* 1998;**508**: 211–221.
12. Liang GH, Xi Q, Leffler CW, Jaggar JH. Hydrogen sulfide activates Ca(2)(+) sparks to induce cerebral arteriole dilatation. *J Physiol* 2012;**590**:2709–2720.
13. Jackson-Weaver O, Osmond JM, Naik JS, Gonzalez Bosc LV, Walker BR, Kanagy NL. Intermittent hypoxia in rats reduces activation of Ca2+ sparks in mesenteric arteries. *Am J Physiol Heart Circ Physiol* 2015;**309**:H1915–H1922.
14. Khavandi K, Baylie RA, Sugden SA, Ahmed M, Csato V, Eaton P, Hill-Eubanks DC, Bonev AD, Nelson MT, Greenstein AS. Pressure-induced oxidative activation of PKG enables vasoregulation by Ca2+ sparks and BK channels. *Sci Signal* 2016;**9**: ra100–ra100.
15. Hu XQ, Song R, Romero M, Dasgupta C, Huang X, Holguin MA, Williams V, Xiao D, Wilson SM, Zhang L. Pregnancy increases Ca(2+) sparks/spontaneous transient outward currents and reduces uterine arterial myogenic tone. *Hypertension* 2019;**73**: 691–702.
16. Essin K, Gollasch M. Role of ryanodine receptor subtypes in initiation and formation of calcium sparks in arterial smooth muscle: comparison with striated muscle. *J Biomed Biotechnol* 2009;**2009**:1–15.
17. Mironneau J, Coussin F, Jeyakumar LH, Fleischer S, Mironneau C, Macrez N. Contribution of ryanodine receptor subtype 3 to Ca2+ responses in Ca2+-overloaded cultured rat portal vein myocytes. *J Biol Chem* 2001;**76**:11257–11264.
18. Ji G, Feldman ME, Greene KS, Sorrentino V, Xin HB, Kotlikoff MI. RYR2 proteins contribute to the formation of Ca(2+) sparks in smooth muscle. *J Gen Physiol* 2004; **123**:377–386.
19. Fritz N, Morel JL, Jeyakumar LH, Fleischer S, Allen PD, Mironneau J, Macrez N. RyR1-specific requirement for depolarization-induced Ca2+ sparks in urinary bladder smooth muscle. *J Cell Sci* 2007;**120**:3784–3791.
20. Matsuki K, Kato D, Takemoto M, Suzuki Y, Yamamura H, Ohya S, Takeshima H, Imaizumi Y. Negative regulation of cellular Ca(2+) mobilization by ryanodine receptor type 3 in mouse mesenteric artery smooth muscle. *Am J Physiol Cell Physiol* 2018; **315**:C1–C9.
21. Fakler B, Adelman JP. Control of K(Ca) channels by calcium nano/microdomains. *Neuron* 2008;**59**:873–881.
22. McCarron JG, Chalmers S, Bradley KN, MacMillan D, Muir TC. Ca2+ microdomains in smooth muscle. *Cell Calcium* 2006;**40**:461–493.
23. Pluger S, Faulhaber J, Furstenau M, Lohn M, Waldschutz R, Gollasch M, Haller H, Luft FC, Ehmke H, Pongs O. Mice with disrupted BK channel beta1 subunit gene feature abnormal Ca(2+) spark/STOC coupling and elevated blood pressure. *Circ Res* 2000; **87**:E53–E60.
24. Lohn M, Lauterbach B, Haller H, Pongs O, Luft FC, Gollasch M. beta(1)-Subunit of BK channels regulates arterial wall[Ca(2+)] and diameter in mouse cerebral arteries. *J Appl Physiol (1985)* 2001;**91**:1350–1354.
25. Lifshitz LM, Carmichael JD, Lai FA, Sorrentino V, Bellve K, Fogarty KE, ZhuGe R. Spatial organization of RYRs and BK channels underlying the activation of STOCs by Ca(2+) sparks in airway myocytes. *J Gen Physiol* 2011;**138**:195–209.
26. Pritchard HAT, Gonzales AL, Pires PW, Drumm BT, Ko EA, Sanders KM, Hennig GW, Earley S. Microtubule structures underlying the sarcoplasmic reticulum support peripheral coupling sites to regulate smooth muscle contractility. *Sci Signal* 2017;**10**: 1–26.
27. Chang K, Xiao D, Huang X, Xue Z, Yang S, Longo LD, Zhang L. Chronic hypoxia inhibits sex steroid hormone-mediated attenuation of ovine uterine arterial myogenic tone in pregnancy. *Hypertension* 2010;**56**:750–757.
28. Chen M, Dasgupta C, Xiong F, Zhang L. Epigenetic upregulation of large-conductance Ca2+-activated K+ channel expression in uterine vascular adaptation to pregnancy. *Hypertension* 2014;**64**:610–618.
29. Pfaffl MW. A new mathematical model for relative quantification in real-time RT-PCR. *Nucleic Acids Res* 2001;**29**:e45.
30. Harraz OF, Abd El-Rahman RR, Bigdely-Shamloo K, Wilson SM, Brett SE, Romero M, Gonzales AL, Earley S, Vigmond EJ, Nygren A, Menon BK, Mufti RE, Watson T, Starreveld Y, Furstenhaupt T, Muellerleile PR, Kurjiaka DT, Kyle BD, Braun AP, Welsh DG. Ca(V)3.2 channels and the induction of negative feedback in cerebral arteries. *Circ Res* 2014;**115**:650–661.
31. Ma Q, Dasgupta C, Li Y, Huang L, Zhang L. MicroRNA-210 suppresses junction proteins and disrupts blood-brain barrier integrity in neonatal rat hypoxic-ischemic brain injury. *Int J Mol Sci* 2017;**18**:1356.
32. Cahill E, Pascoli V, Trifilieff P, Savoldi D, Kappes V, Luscher C, Caboche J, Vanhoutte P. D1R/GluN1 complexes in the striatum integrate dopamine and glutamate signalling to control synaptic plasticity and cocaine-induced responses. *Mol Psychiatry* 2014;**19**: 1295–1304.
33. Brenner R, Perez GJ, Bonev AD, Eckman DM, Kosek JC, Wiler SW, Patterson AJ, Nelson MT, Aldrich RW. Vasoregulation by the beta1 subunit of the calcium-activated potassium channel. *Nature* 2000;**407**:870–876.
34. Tanaka Y, Koike K, Alioua A, Shigenobu K, Stefani E, Toro L. Beta1-subunit of MaxiK channel in smooth muscle: a key molecule which tunes muscle mechanical activity. *J Pharmacol Sci* 2004;**94**:339–347.
35. Hu XQ, Zhang L. Function and regulation of large conductance Ca(2+)-activated K+ channel in vascular smooth muscle cells. *Drug Discov Today* 2012;**17**:974–987.
36. Ledoux J, Werner ME, Brayden JE, Nelson MT. Calcium-activated potassium channels and the regulation of vascular tone. *Physiology (Bethesda)* 2006;**21**:69–78.
37. Jaggar JH, Porter VA, Lederer WJ, Nelson MT. Calcium sparks in smooth muscle. *Am J Physiol Cell Physiol* 2000;**278**:C235–C256.
38. Perez GJ, Bonev AD, Nelson MT. Micromolar Ca(2+) from sparks activates Ca(2+)-sensitive K(+) channels in rat cerebral artery smooth muscle. *Am J Physiol Cell Physiol* 2001;**281**:C1769–C1775.
39. Cox DH, Aldrich RW. Role of the beta1 subunit in large-conductance Ca(2+)-activated K(+) channel gating energetics. Mechanisms of enhanced Ca(2+) sensitivity. *J Gen Physiol* 2000;**116**:411–432.
40. Pritchard HAT, Pires PW, Yamasaki E, Thakore P, Earley S. Nanoscale remodeling of ryanodine receptor cluster size underlies cerebral microvascular dysfunction in Duchenne muscular dystrophy. *Proc Natl Acad Sci USA* 2018;**115**:E9745–E9752.
41. Leo MD, Zhai X, Muralidharan P, Kuruvilla KP, Bulley S, Boop FA, Jaggar JH. Membrane depolarization activates BK channels through ROCK-mediated beta1 subunit surface trafficking to limit vasoconstriction. *Sci Signal* 2017;**10**: 1–9.
42. Kaßmann M, Szijártó IA, García-Prieto CF, Fan G, Schleifenbaum J, Anistan Y-M, Tabeling C, Shi Y, Le Noble F, Witzenrath M, Huang Y, Markó L, Nelson MT, Gollasch M. Role of ryanodine type 2 receptors in elementary Ca(2+) signaling in arteries and vascular adaptive responses. *J Am Heart Assoc* 2019;**8**:e010090.
43. LöHn M, Jessner W, FüRstenau M, Wellner M, Sorrentino V, Haller H, Luft FC, Gollasch M, Regulation of calcium sparks and spontaneous transient outward currents by RyR3 in arterial vascular smooth muscle cells. *Circ Res* 2001;**89**:1051–1057.
44. Yang XR, Lin MJ, Yip KP, Jeyakumar LH, Fleischer S, Leung GP, Sham JS. Multiple ryanodine receptor subtypes and heterogeneous ryanodine receptor-gated Ca2+ stores in pulmonary arterial smooth muscle cells. *Am J Physiol Lung Cell Mol Physiol* 2005; **289**:L338–L348.
45. Kinnear NP, Wyatt CN, Clark JH, Calcraft PJ, Fleischer S, Jeyakumar LH, Nixon GF, Evans AM. Lysosomes co-localize with ryanodine receptor subtype 3 to form a trigger zone for calcium signalling by NAADP in rat pulmonary arterial smooth muscle. *Cell Calcium* 2008;**44**:190–201.
46. Vaithianathan T, Narayanan D, Asuncion-Chin MT, Jeyakumar LH, Liu J, Fleischer S, Jaggar JH, Dopico AM. Subtype identification and functional characterization of ryanodine receptors in rat cerebral artery myocytes. *Am J Physiol Cell Physiol* 2010;**299**: C264–C278.
47. Zhao G, Zhao Y, Pan B, Liu J, Huang X, Zhang X, Cao C, Hou N, Wu C, Zhao KS, Cheng H. Hypersensitivity of BKCa to Ca2+ sparks underlies hyporeactivity of arterial smooth muscle in shock. *Circ Res* 2007;**101**:493–502.
48. Schwanhausser B, Busse D, Li N, Dittmar G, Schuchhardt J, Wolf J, Chen W, Selbach M. Global quantification of mammalian gene expression control. *Nature* 2011;**473**: 337–342.
49. Vogel C, Marcotte EM. Insights into the regulation of protein abundance from proteomic and transcriptomic analyses. *Nat Rev Genet* 2012;**13**:227–232.
50. Liu Y, Beyer A, Aebersold R. On the dependency of cellular protein levels on mRNA abundance. *Cell* 2016;**165**:535–550.
51. Coussin F, Macrez N, Morel JL, Mironneau J. Requirement of ryanodine receptor subtypes 1 and 2 for Ca(2+)-induced Ca(2+) release in vascular myocytes. *J Biol Chem* 2000;**275**:9596–9603.

52. Zieman SJ, Melenovsky V, Kass DA. Mechanisms, pathophysiology, and therapy of arterial stiffness. *Arterioscler Thromb Vasc Biol* 2005;**25**:932–943.
53. Barbado M, Fablet K, Ronjat M, De Waard M. Gene regulation by voltage-dependent calcium channels. *Biochim Biophys Acta* 2009;**1793**:1096–1104.
54. Nieves-Cintron M, Amberg GC, Nichols CB, Molkentin JD, Santana LF. Activation of NFATc3 down-regulates the beta1 subunit of large conductance, calcium-activated K+ channels in arterial smooth muscle and contributes to hypertension. *J Biol Chem* 2007;**282**:3231–3240.
55. Jordan T, Jiang H, Li H, DiMario JX. Inhibition of ryanodine receptor 1 in fast skeletal muscle fibers induces a fast-to-slow muscle fiber type transition. *J Cell Sci* 2004;**117**:6175–6183.
56. Gomez MF, Stevenson AS, Bonev AD, Hill-Eubanks DC, Nelson MT. Opposing actions of inositol 1,4,5-trisphosphate and ryanodine receptors on nuclear factor of activated T-cells regulation in smooth muscle. *J Biol Chem* 2002;**277**:37756–37764.

Translational perspective

A successful pregnancy requires adequate uterine vascular adaptation. The present study demonstrates that pregnancy-induced RyR1 and RyR2 upregulation in uterine arteries exerts their regulatory role on uterine arterial myogenic tone via impacting the Ca^{2+} spark-STOC coupling, BK_{Ca} β1 expression, and association of BK_{Ca} β1 and BK_{Ca} α. Our findings reveal a crucial role of the RyRs-BK_{Ca} channel partnership in mediating pregnancy-induced uterine vascular adaptation. Thus, our findings provide valuable insights into understanding the mechanisms underlying uterine vascular adaptation in pregnancy.